JOURNAL OF MATERIALS SCIENCE **36** (2001) 1271–1276

Synthesis and properties of copper and samarium doped yttria-bismuth oxide powders and membranes

Y. ZENG, Y. S. LIN
Department of Chemical Engineering, University of Cincinnati, Cincinnati, Ohio 45221, USA

Powders of $Bi_{1.5}Y_{0.5-y}Cu_yO_{3-\delta}$ (BYC) and $Bi_{1.5}Y_{0.3}Sm_{0.2}O_3$ in the fluorite phase structure were prepared by the citrate method. The chemical reactions involved in the synthesis of these powders were proposed and verified experimentally. Dense BYC and BYS membranes were prepared from the powders by the press and sintering method. The optimum conditions for powder preparation as well as for membrane fabrication were determined in this study with the aid of various characterization methods. The BYC and BYS membranes were gas-tight to helium. These doped bismuth-yttrium (BY) oxide membranes show similar ionic conductivity but much higher oxygen permeability (electronic conductivity) as compared to the undoped BY membrane.

1. Introduction

Fluorite structured bismuth oxide (δ-Bi_2O_3) has been known as a good ionic conductor at temperatures higher than 750°C. However, due to its low melting point (~810°C) and electronic conductivity, it is not feasible to utilize pure Bi_2O_3 as an oxygen permeable membrane for high temperature applications. Research efforts were reported to stabilize δ-phase Bi_2O_3 to lower temperatures (500–700°C) by doping certain amount (20–35 mol%) of appropriate metal oxide, such as yttria and erbia [1, 2]. Although such attempt was later proved unsuccessful [3], yttria or erbia doped Bi_2O_3 could find applications at higher temperatures since their melting points are about 200°C higher than that of pure Bi_2O_3.

Recently we found that the yttria doped bismuth oxide (BY) in the fluorite structure has excellent catalytic properties for oxidative coupling of methane (OCM) [4, 5]. The results show possibility of using this material as membrane in a membrane reactor to substantially improve the selectivity and yield for the important OCM reaction [6]. Two problems that need to be solved before BY can be used in the membrane reactor for OCM. First, BY is not stable under highly reducing and reactive environment, such as methane. The chemical stability of BY should be improved. Second, due to its low electronic conductivity, dense BY membrane has relatively low oxygen permeation flux [7]. Therefore, it is important to increase its electronic conductivity in order to achieve higher oxygen permeability. It was shown that doping Sm_2O_3 and CuO into BY could improve respectively the chemical stability and electronic conductivity of BY ceramic [8, 9]. The present paper is focused on citrate synthesis and properties of Sm_2O_3 and CuO doped BY powders and membranes.

2. Experimental

The citrate (Pecchini) method [10] was used to prepare powders of solid solution of $Bi_{1.5}Y_{0.5-y}Cu_yO_3$ (abbreviated as **BYC**) and $Bi_{1.5}Y_{0.5-y}Sm_yO_3$ (with $y = 0.2$ only, abbreviated as **BYS**). Preliminary work showed that it was difficult to obtain single phase, fluorite-structured solid solution of BYS and BYC with y larger than 0.2. Therefore, the study was focused on BYS and BYC with highest possible Cu or Sm concentration. BYC in three compositions ($y = 0.2$, 0.1, 0.05), abbreviated as BYC20, BYC10 and BYC5 respectively, were prepared in order to investigate the effects of dopant concentration on preparation of this group of materials.

In synthesis of the powders, stoichiometric amounts of the corresponding metal nitrates, i.e., $Bi(NO_3)_3 \cdot 5H_2O$ (99%, Fisher), $Y(NO_3)_3 \cdot 6H_2O$ (99.5%, Alpha) and $Cu(NO_3)_3 \cdot 2.5H_2O$ (98%, Fisher) or $Sm(NO_3)_3 \cdot 6H_2O$ (99.9%, Alpha), were fully dissolved in a dilute nitric acid solution (10 vol% of concentrated HNO_3), followed by addition of citric acid (99%, Fisher). A transparent solution was obtained and subsequently heated while stirring to temperature about 90–110°C. After the system was kept isothermally with reflux and stirring for a certain amount of time, water was removed from the system by evaporation until a sticky gel-like solid was formed. It should be noted that the above experiment must be conducted in a fume hood due to the emission of hazardous chemicals.

The above-mentioned gel was dried in air overnight. The dried polymeric gel was accurately weighed in order to study the chemical reactions occurred during the polymerization and condensation periods. It was then placed in a box furnace which had been pre-heated to 400°C. A thermal couple was attached to the sample

to monitor the instantaneous temperature change inside the sample. Self-ignition of the sample took place when it reached a certain temperature. The weight change during this period was studied by using a high temperature microbalance (Cahn 1000). After self-ignition, this powder was further calcined at 600–750°C for a certain period of time to obtain a yellowish (for BYS) or gray to black (for BYC) powder, which is referred to as green powder in this study.

The above-mentioned green powders were packed in a stainless steel mold (26.5 mm in diameter) and uniaxially pressed into the disk shape by imposing a hydraulic pressure, ranging from 20 to 160 MPa. The densities of the green disks were calculated from their weights and dimensions (accuracy: ±0.05 mm). The green disks were sintered at 825–1100°C for 1–60 h with a heating/cooling rate of 5°C/min.

The bulk densities of the final BYC and BYS disks were obtained by using the same method applied for the green disks while their real (or skeleton) densities were measured by the Archemedes method using DI water as the immersion liquid. Phase structure and the crystallinity of the samples obtained in each step after the self-ignition process were investigated by the X-ray diffraction measurement (Siemens Kristalloflex D500 diffractometer, with CuK_α radiation). The theoretical densities of the samples were calculated from the *d*-spacing values in their XRD patterns. The grain size (micro-structure) of the samples formed in each step of the preparation process were examined by SEM.

Gas tightness of the membrane disks was tested by helium permeation in a permeation system at room temperature using vacuum grease as sealant. Oxygen permeation through these membranes was measured in the same permeation system at temperatures higher than 650°C, using a homemade Bi_2O_3-based sealant [11]. The electrical conductivities of the membrane disks were obtained with the four point DC conductivity measurement method [12].

3. Results and discussion

3.1. Material synthesis chemistry

In the citrate method polymerization reactions between citric acid and metal ions were taking place during the first isothermal reflux period, as suggested by Lessing [13]. Otherwise, metal citrates would be formed and precipitated out of the solution since they are insoluble in water. In the present experiments, no sedimentation was observed and the solution was transparent during the whole period of the synthesis experiment when the conditions were properly controlled. It is generally believed that the metal ions are chelated with citric acid through -OH and -COOH groups and served as the bridges between the citric acid molecules to form polymeric molecules. Direct polymerization between citric acid molecules could also take place. Such formed polymers are soluble in water since they contain a considerable amount of hydrophilic groups, such as: -OH and -COOH. These polymerization reactions can be illustrated by reaction shown in Fig. 1A.

During water removing period, the above mentioned system became more and more sticky and viscous,

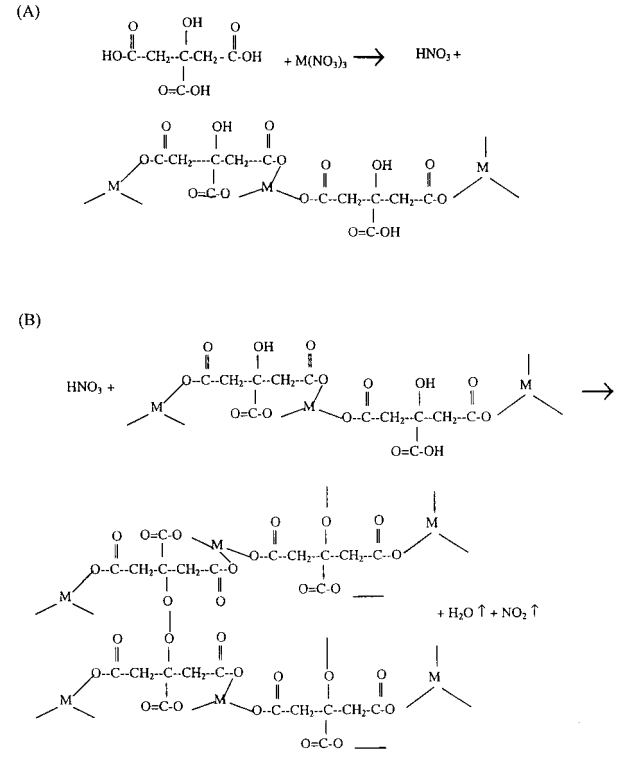

Figure 1 Polymerization reactions in the initial stage (A) and water removal stage (B) of the citrate process (M represents metal ions, such as bismuth, yttrium, copper or samarium).

and finally turned into a gel-like solid with a color of light blue (for BYC) or white (for BYS). This phenomenon strongly suggests that reactions occurred between the previously formed polymeric molecules via -COH and HOC-condensation, forming a big chuck of cross-linked, gel-like polymer. The removal of water out of the system had also favored these reactions. At the time when nearly all the water was evaporated, a brownish gas bubbled out of the sticky gel, resulting in a large expansion in the solid volume. The solid thus became very porous. This is caused by the decomposition of nitric acid in the system into NO_2. The overall reaction during this period is represented by reaction shown in Fig. 1B.

The above-mentioned gel-like material was dried in air. The theoretic weight of this dried sample was also calculated from reactions shown in Fig. 1 by knowing the initial amount of the precursors, i.e., metal nitrates and citric acid, and assuming that all the -COOH and -COH groups in citric acid were ether chelated with metal ions or self-condensed to generate water. The real sample weight was close to the theoretical one within ±4%. This further verifies that the above polymerization and condensation reaction indeed took place during the citrate process.

Fig. 2 shows the bulk temperature in BYC sample as a function of time during the self-ignition period. With the oven temperature at 400°C, the sample temperature increased quickly from room temperature to about 100°C due to the large temperature difference between the sample and oven. After that, the increase in the sample temperature became slower as the temperature difference became smaller. However, when the sample temperature reached about 250°C, it suddenly increased

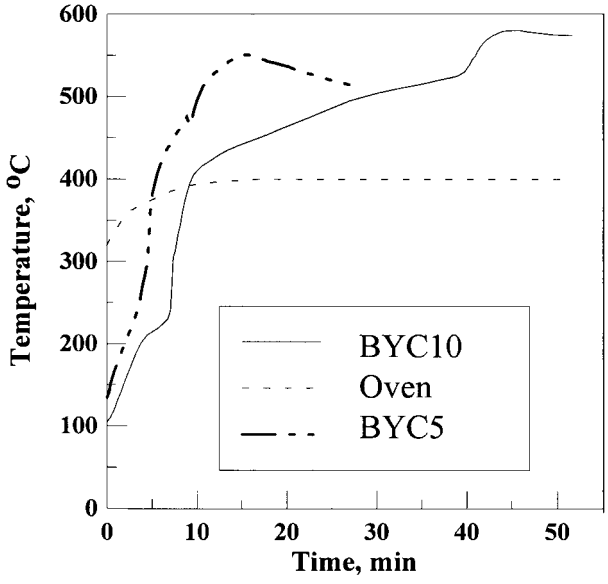

Figure 2 Sample temperature as a function of time during self-ignition period.

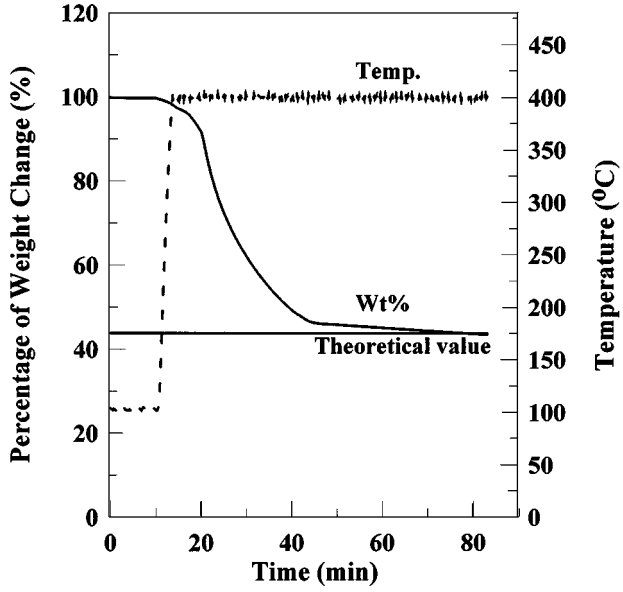

Figure 4 BYC20 sample weight as a function of time during self-ignition period.

to more than 400°C at very fast rate. This indicates that self-ignition reactions started and generated a considerable amount of heat. After sample temperature was higher than 420°C, it increased at a much lower rate and eventually leveled off at 550–580°C. The whole period lasted for 30–50 min, as indicated by the temperature and sample appearance. This primarily depended on the sample amount and the rate of oxygen transport from the gas phase to the ignition reaction. The charred sample was so loose that its volume was about 4 times that of the original dried gel. Its color ranged from light green to black as the copper content increased. Similar temperature change was also found for BYS sample during its self-ignition period as shown in Fig. 3.

The self-ignition reaction is relatively simple and can be described by the following reaction:

$$\text{Polymeric Gel} + O_2 \rightarrow \alpha\text{-}Bi_{2-x}M'_xO_3 + \delta\text{-}Bi_{2-x}M'_xO_3 + C + CO_2 \uparrow + H_2O \uparrow$$

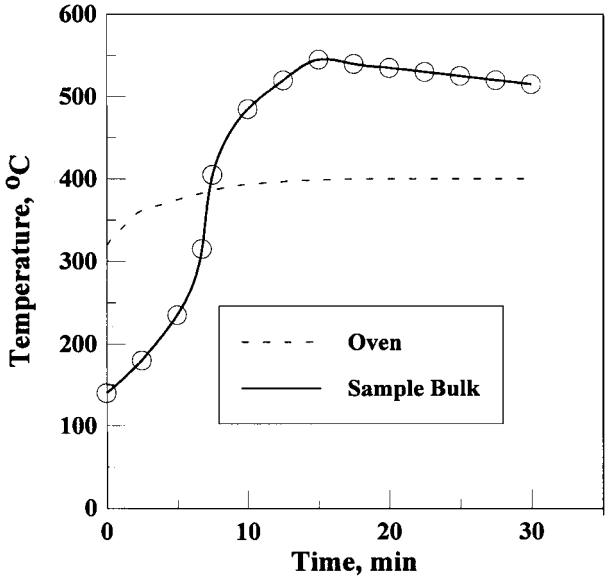

Figure 3 BYS sample temperature as a function of time during self-ignition period.

As revealed by XRD measurement, the major phase of the metal oxides formed after the self-ignition period was α-Bi_2O_3 phase with minor δ-Bi_2O_3 phase. No phases of CuO, Sm_2O_3, Y_2O_3 or Cu and Sm metals, were observed in the XRD patterns. This indicates that the solid solutions of Bi_2O_3 phases doped with Y and Cu or Sm ions were formed after self-ignition.

The sample weight change during the self-ignition period was studied by an experiment carried out in the Cahn electronic microbalance. The results for a BYC sample are illustrated in Fig. 4. After about 2 g dried gel was mounted in the sample pan of the balance, the system was heated up to 400°C at a very fast rate. As shown in Fig. 4, sample weight decreased exponentially with time and eventually reached a constant value after about 30–40 min. The sample maintained 45% of its original weight. This is very close to the theoretical value which was calculated with the assumption that the dried gel had a molecular structure given in Fig. 1B and the majority of carbon and metal atoms in the gel respectively became CO_2 and metal oxides after self-ignition. After calcination at 600–800°C for 3 h, the carbon remained in the charred powder was removed by combustion reaction and all the α-phase Bi_2O_3 was completely transferred to δ-phase as confirmed by the XRD analysis. The chemical and phase-structural change of the sample can be described as:

$$\alpha\text{-}Bi_{2-x}M'_xO_3 + \delta\text{-}Bi_{2-x}M'_xO_3 + C + O_2 \rightarrow \delta\text{-}Bi_{2-x}M'_xO_3 + CO_2 \uparrow$$

3.2. Optimum synthesis conditions

Since hydrolysis of $Bi(NO_3)_3$ and $Y(NO_3)_3$ was found to take place in water, dilute nitric acid was used to dissolve metal nitrates to avoid the formation of the $Bi(OH)_3$ and $Y(OH)_3$ precipitates. The minimum concentration was found to be 10 vol% of concentrated nitric acid. To make 0.031 mol of BYC, at least 400 ml of such diluted nitric acid is requied to fully dissolve

the corresponding amount of metal nitrates and citric acid. The molar amount of the citric acid was 1.5 times that of the total metal ions in order to ensure that all the metal ions are chelated into the polymer structure. The optimum temperature for polymerization period was found to be 90–110°C. For temperature lower than 80°C, metal citrates were formed and precipitated from the solution, resulting in a white, unclear suspension. In this case, polymerization reactions would not take place. It took at least 3 h for polymerization reactions to be finished.

The solvent was removed by drying the gel at 100–110°C overnight. The dried gel showed continuous fibers with irregular pores in between. It was not necessary to grind the dried sample into powder before self-ignition, since it had a very porous structure good for transport of oxygen and self-ignition. Although the polymer sample started to be pyrolyzed at 250°C as observed in Figs 2 and 3, it was not combusted with glow and flame until 350°C. Therefore, in order to fulfill a fast and uniform self-ignition without pyrolysis, oven was pre-heated to 400 °C. The ignition time was selected as 1 h. It was noted that a fast supply of air into the system was very important.

The powders after self-ignition contained particle aggregates (BYS or BYC solid solution) and some fibers in relatively larger size (carbon residuals). The particles inside the aggregates were smaller than 0.1 μm. The charred sample was ground into powder with an agate mortar and peddle. The powder was then calcined at 600–800°C for 3 h, during which the carbon residual was decomposed and the δ-phase was formed. The green powders after calcination consisted of aggregates with sizes of 3–8 μm. The aggregates were porous and contained particles smaller than 0.5 μm. It was found that the calcined powder had worse sinterability when higher temperature and longer time were used in the calcination due to the formation of larger grains and particles. The best calcination temperatures were 750°C for BYC samples and 800°C for BYS sample.

The green powders were packed into a stainless steel mold and pressed into disk shape with hydraulic pressure. Figs 5 and 6 show the effect of pressing pressure on the densities of BYC and BYS green disks. The density of both sample increased exponentially with increasing pressure and leveled off at about 100 MPa. As shown in Fig. 7, the effect of pressing pressure on the density of sintered disk followed a similar trend as that for the density of green disk. Therefore, the optimum pressing pressure was selected as 100 MPa for both samples. It is worthy to mention here that BYC powders were generally more difficult to be pressed into an integral disk than BYS powder. It was also found that addition of appropriate amount of water into both green powders would improve the pressing performance, on both density and integrity of disks. The amount of water added was 10–20 wt% of dried green powder.

Beside pressing pressure, sintering temperature and time have significant effects on the properties of the final disks. It was found that the sintering temperature played a more important role than the sintering time. The sintering temperatures for the BYC disks with different compositions were selected to be 20–30°C

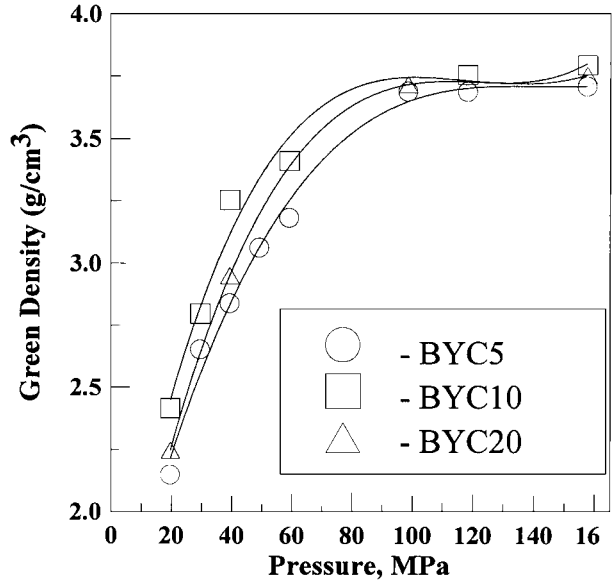

Figure 5 Effect of pressing pressure on the densities of BYC green disks.

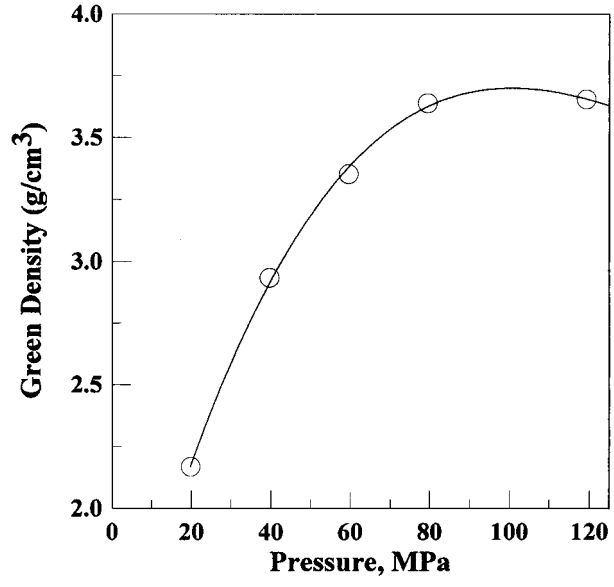

Figure 6 Effect of pressing pressure on the densities of BYC green disk.

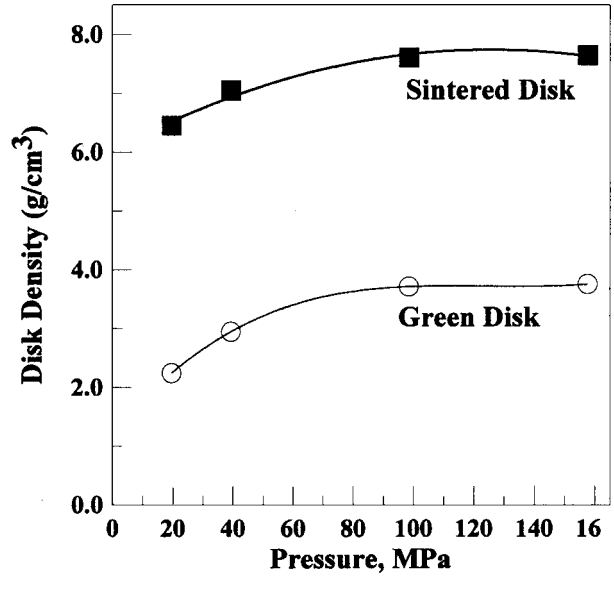

Figure 7 Effect of pressing pressure on the densities of sintered BYC20 membrane disks.

lower than their melting points to avoid possible sample melting and partial segregation of CuO from the solid solution. Therefore, the sintering temperature for BYC20, BYC10 and BYC5 were respectively 825, 875 and 900°C and that for BYS was 1050 °C. The sintering time was selected as 48 h for all samples to ensure a complete sintering.

3.3. Material and membrane properties

Fig. 8 presents the XRD patterns of BYC10 powder and final disk. As shown, the major phase in the green powder was δ-Bi_2O_3 phase while the final sintered disk was in a perfect δ-phase structure with relatively larger grain size as indicated by its sharp peaks. Fig. 9 shows the XRD patterns of a BYS sample. The green powder of BYS sintered at 600°C for 3 h contained a considerable amount of α-Bi_2O_3 phase and carbon residual. For BYS the α-Bi_2O_3 phase transformed to δ-Bi_2O_3 phase at higher temperature (about 800°C), as compared to BYC. For this reason and also because of its higher melting point, BYS disk was sintered at a higher temperature (1050°C) than BYC disk. As shown in Fig. 9, the sintered BYS disk also has the perfect fluorite structure.

For BYC disks, both real and theoretical densities were found to decrease with increasing copper content. At the optimum preparation conditions the relative densities of BYC disks were larger than 95%. For example, the real and theoretical densities of a BYC10 disk were respectively 7.76 and 8.17 g/cm^3. For BYS membrane made of green powder calcined at 800°C for 3 h, pressed with 120 MPa and sintered at 1050°C for 48 h, its real and theoretical densities were respectively 8.02 and 8.10 g/cm^3, i.e., with a relative density of 99%.

Gas permeation tests showed that helium was impermeable through the membrane disks at temperatures ranging from the room temperature to 850°C (for BYC) or 1000 °C (for BYS), indicating a complete gas-tightness for both membranes. Oxygen permeation flux through BYC and BYS membranes were measured at 650–850°C with an oxygen partial pressure gradient of 0.21 atm and $5 \times 10^{-4} - 1 \times 10^{-3}$ atm [11]. For 2 mm thick BYC10 and BYS membranes, the oxygen flux is respectively 6.1×10^{-9} and 7.5×10^{-9} mol/cm^2.s at 800°C. The oxygen permeability of BYC and BYS membranes is about 5 to 10 times that of yttria- or erbia-bismuth oxide membrane without being doped with copper or samarium [7, 11]. Since for the oxygen ionic conductor the oxygen permeability is determined by the electron-conductivity [11], this improvement in oxygen permeability indicates that doping copper or samarium has substantially improved the electronic conductivity of the bismuth oxide based ceramics.

Electric (oxygen ionic) conductivity of BYC and BYS membranes was measured by the four point DC

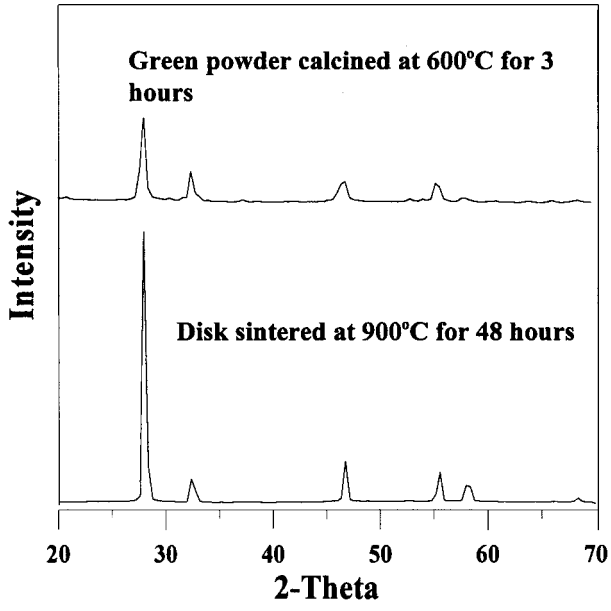

Figure 8 XRD patterns of BYC10 green powder and final disk.

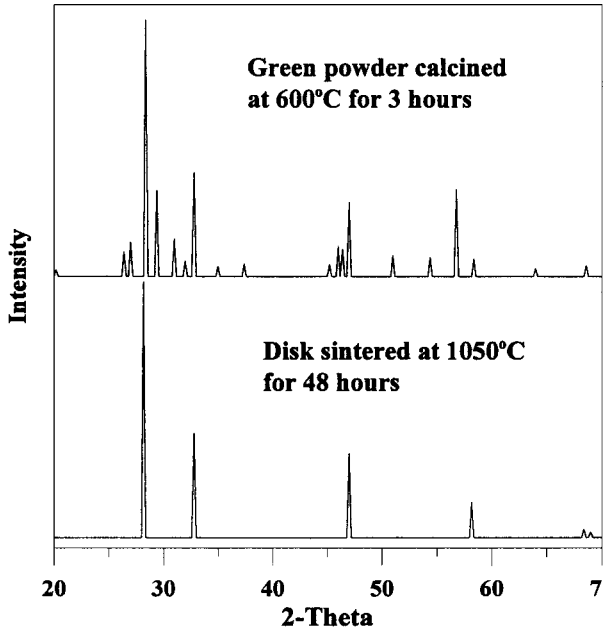

Figure 9 XRD patterns of BYS green powder and final disk.

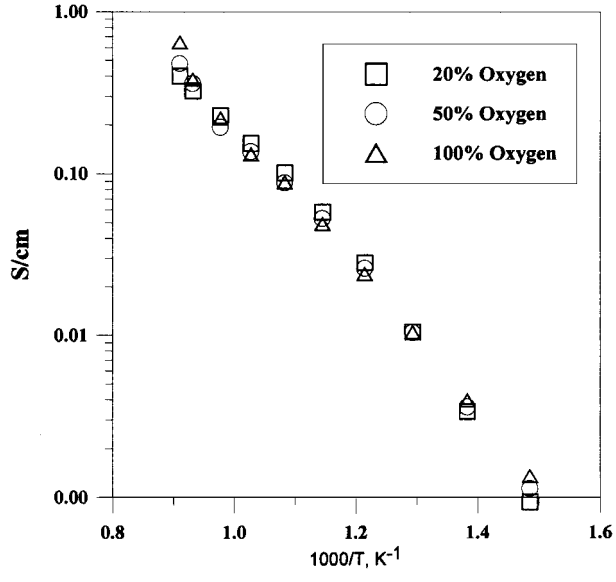

Figure 10 Electric conductivity of BYC20 membrane as function of temperature.

TABLE I Comparison of conductivities of different Bi_2O_3-based materials

Material	Ea (kJ/mol)		Conductivity (S/cm)			Ref.
	low temp.	high temp.	500°C	600°C	700°C	
BYC20	100.2	66.9	1.05×10^{-2}	5.82×10^{-2}	0.154	this work
BYS	98.3	66.6	1.11×10^{-2}	6.79×10^{-2}	0.197	this work
$Bi_{1.5}Y_{0.5}O_3$	103.3	63.7	1.2×10^{-2}	N/A	0.16	[1]
$Bi_{0.8}Y_{0.1}Nb_{0.1}O_{1.5}$	121.7	95.6	1.4×10^{-2}	5.7×10^{-2}	0.19	[14]

TABLE II Conduction activation energy for BYC20 sample

P_{O2} (atm)	0.2	0.5	1
E_a (<600 °C)	100.2	95.3	88.1
E_a (>600 °C)	66.9	76.1	86.1

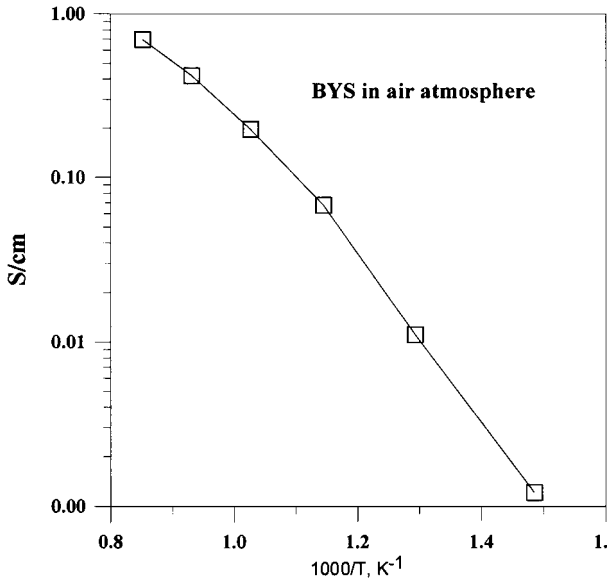

Figure 11 Electric conductivity of BYS membrane as function of temperature.

method in the temperature range of 400–900°C. Results are presented in Fig. 10 and Fig. 11. The electric conductivity data for the BYC and BYS samples are very similar and increase exponentially with increasing temperature. There is a transition at 600°C for the temperature dependency of the electric conductivity for both BYS and BYC samples. The electric conductivity shows a higher activation energy below 600°C. The change in activation energy could be a result of order-disorder transition of the oxygen vacancy in the BY based ceramics at 600°C. Table I compares the reported conductivity and activation energy of BY and BYN_d oxides [1, 14] with those of BYC and BYS oxides of this study. All data are very close in spite of different dopants in the samples.

The electric conductivity of these oxides is dominated by their ionic conductivity. Since BY, BYS and BYC have same oxygen defect crystal structure as pure Bi_2O_3, they should have similar oxygen ion conduction properties. As shown in Fig. 10, oxygen partial pressure has some, but small effect on the conductivity of BYC oxide. Table II lists the activation energy for electric (oxygen ionic) conduction in the BYC sample in these two temperature ranges at different oxygen partial pressures. It is interesting to note that the transition in the activation energy becomes less obvious at higher oxygen partial pressure, as shown in Table II.

4. Summary

Optimum conditions were identified for synthesis of powders of $Bi_{1.5}Y_{0.5-y}Cu_yO_3$ ($y < 0.2$) (BYC) and $Bi_{1.5}Y_{0.3}Sm_{0.2}O_3$ (BYS) in the fluorite structure. The powder synthesis process involved polymerization and chelating reactions resulting in uniform mixing of different metal ions in the atomic scale. Solid solution is formed right after the self-ignition step. Gas-tight dense BYC and BYS membranes with relative density respectively higher than 95% and 99% were prepared from the powder prepared by the citrate method. BYC and BYS membranes have oxygen permeability about five- to ten-fold that of BY membranes.

References

1. T. TAKAHASHI, H. IWAHARA and T. ARAO, *J. Appl. Electrochem.* **5** (1975) 187.
2. T. C. YUAN and A. V. VIRKAR, *J. Amer. Ceram. Soc.* **71** (1988) 451.
3. A. V. JOSHI, S. KULKARNI, J. NACHLAS, J. DIAMOND, N. WEBER and A. V. VIRKAR, *J. Mater. Sci.* **25** (1990) 1237.
4. Y. ZENG and Y. S. LIN, *Applied Catalysis* A **159** (1997) 101.
5. *Idem., J. Catal.* **182** (1999) 30.
6. W. WANG and Y. S. LIN, *J. Membrane Sci.* **103** (1995) 219.
7. H. J. M. BOUWMEESTER, H. KRUIDHOF, A. J. BURGGRAAF and P. J. GELLINGS, *Solid State Ionics* **53–56** (1992) 460.
8. Y. ZENG, Ph.D. Thesis, University of Cincinnati, Cincinnati, Ohio 1998.
9. M. LIU, A. V. JOSHI, Y. SHEN and K. KRIST, U.S. Patent no., 5,273,628 (1993).
10. M. P. PECHINI, U.S. Patent no., 3,330,697 (1967).
11. J. HAN, Y. ZENG and Y. S. LIN, *J. Membr. Sci. J. Membrane Sci.* **132** (1997) 235.
12. X. QI and Y. S. LIN, *Solid State Ionics* **120** (1999) 85.
13. P.A. LESSING, *Am. Ceram. Soc. Bull.* **68** (5) (1989) 1002.
14. G. MENG, C. CHEN, X. HAN, P. YANG and D. PENG, *Solid State Ionics* **28–30** (1988) 533.

Received 18 January
and accepted 3 August 2000